HOKKAIDO UNIVERSITY

Title	Effective Oxidation of 5-Hydroxymethylfurfural to 2,5-Diformylfuran by an Acetal Protection Strategy
Author(s)	Boonyakarn, Tat; Wiesfeld, Jan J.; Asakawa, Miyuki; Chen, Lulu; Fukuoka, Atsushi; Hensen, Emiel J. M.; Nakajima, Kiyotaka
Citation	ChemSusChem, 15(7), e202200059 https://doi.org/10.1002/cssc.202200059
Issue Date	2022-04-07
Doc URL	http://hdl.handle.net/2115/89329
Rights	This is the peer reviewed version of the following article: [T. Boonyakarn, J. J. Wiesfeld, M. Asakawa, L. Chen, A. Fukuoka, E. J. M. Hensen, K. Nakajima, ChemSusChem 2022, 15, e202200059.], which has been published in final form at [https://doi.org/10.1002/cssc.202200059]. This article may be used for non-commercial purposes in accordance with Wiley Terms and Conditions for Use of Self-Archived Versions. This article may not be enhanced, enriched or otherwise transformed into a derivative work, without express permission from Wiley or by statutory rights under applicable legislation. Copyright notices must not be removed, obscured or modified. The article must be linked to Wiley ' s version of record on Wiley Online Library and any embedding, framing or otherwise making available the article or pages thereof by third parties from platforms, services and websites other than Wiley Online Library must be prohibited.
Type	article (author version)
File Information	Manuscript_revised.pdf

Instructions for use

Hokkaido University Collection of Scholarly and Academic Papers : HUSCAP

RESEARCH ARTICLE

Effective Oxidation of (5-Hydroxymethyl)furfural to 2,5-Diformylfuran by an Acetal Protection Strategy

Tat Boonyakarn,[a] Jan J. Wiesfeld,[a] Miyuki Asakawa,[a] Lulu Chen,[b] Atsushi Fukuoka,[a] Emiel J.M. Hensen,[b] and Kiyotaka Nakajima*[a]

[a] T. Boonyakarn, Dr. J.J. Wiesfeld, M. Asakawa, Prof. Dr. A. Fukuoka, Prof. Dr. K. Nakajima
Institute for Catalysis
Hokkaido University
Kita 21 Nishi 10, Kita-ku, Sapporo 001-0021, Japan.
E-mail: nakajima@cat.hokudai.ac.jp
[b] L. Chen, Prof. Dr. Ir. E. J.M. Hensen
Laboratory of Inorganic Chemistry and Catalysis, Department of Chemical Engineering and Chemistry
Eindhoven University of Technology
PO Box 513, 5600 MB Eindhoven, The Netherlands

Supporting information for this article is given via a link at the end of the document

Abstract: An acetal protection strategy for (5-hydroxymethyl)furfural (HMF) was used to obtain 2,5-diformyfuran (DFF) using concentrated HMF solutions and a γ-Al_2O_3-supported Ru catalyst (Ru/γ-Al_2O_3). The HMF-acetal with 1,3-propanediol can be oxidized to DFF-acetal with a yield of 84.0% at an HMF conversion of 94.2% from a 50 wt% solution. In contrast, aerobic oxidation of nonprotected HMF using a 10 wt% solution afforded DFF only in a moderate yield (52.3%). Kinetic studies indicate that the six-membered ring acetal group not only prevents side reactions but also accelerates aerobic oxidation of the -CH_2OH moiety to -CHO under retention of the acetal functionality. Organic deposits formed during the reaction explained the significant decrease in the activity of the Ru/γ-Al_2O_3 catalyst, which could be recovered neither by washing in water or organic solvents, nor by a calcination-reduction treatment. Sonication of the used Ru/γ-Al_2O_3 catalyst in an aqueous NaOH solution successfully removed the deposits and allowed reuse of the catalyst for at least four times without activity loss.

Introduction

Lignocellulosic biomass is widely regarded as an abundant, easily accessible and renewable carbon resource that can replace fossil fuels.[1,2] Catalytic valorization of its main constituents (cellulose, hemicellulose, and lignin) into platform molecules has been extensively studied to realize sustainable production of fuels and commodity chemicals.[3–7] Hydrolysis of cellulose into glucose and its subsequent dehydration lead to (5-hydroxymethyl)furfural (HMF),[8–14] which is a versatile intermediate for production of a wide range of chemicals and fuel additives. Scheme 1 presents reaction paths for the conversion of HMF to intermediates that can be used as monomers for manufacture of polymers with a reduced carbon footprint. Aerobic oxidation of the two functional groups in HMF affords 2,5-furandicarbocylic acid (FDCA),[15–19] while hydrogenation of HMF yields 2,5-bis(hydroxymethyl)furan (BHMF)[20–23] and 2,5-(bis(hydroxymethyl)tetrahydrofuran (BHMTHF).[24–28] BHMTHF can be further transformed to aliphatic alcohols such as 1,6-hexanediol and 1,2,6-hexanetriol, and 1,6-hexanediol is a source of adipic acid.[24,29–31] Partial oxidation of HMF can also lead to 2,5-diformylfuran (DFF), which can be further converted to 2,5-bis(aminomethyl)furan (AMF).[32–36] Although AMF has substantial potential as a building block for polyamides,[37,38] efficient synthetic procedures have not yet been developed. For the first step of AMF production, we have studied aerobic oxidation of the hydroxymethyl group in HMF to the corresponding formyl group using supported metal catalysts and concentrated solutions (Scheme 1).

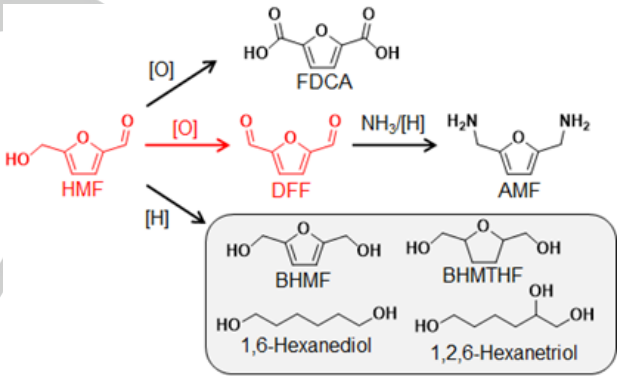

Scheme 1. Reaction pathways to several valuable monomers obtainable from HMF.

Reaction paths for the aerobic oxidation of HMF to FDCA in water are illustrated in Scheme S1. The formyl group is easily oxidized to the corresponding carboxylic acid in water via the formation of a geminal diol intermediate. HMF can be easily oxidized to FDCA through 5-(hydroxymethyl)furan-2-carboxylic acid (HMFCA) and 5-formylfuran-2-carboxylic acid (FFCA) as intermediates, while DFF is only obtained in very small amounts. The use of non-protic organic solvents such as toluene and N,N'-dimethylformamide (DMF) prevents the hydration of the formyl group to a geminal diol (Scheme S1) and its subsequent oxidative dehydrogenation to a carboxylic acid. This provides an opportunity to selectively oxidize HMF to DFF. Supported noble metal catalysts such as Pt, Pd, Au, or Ru have been extensively studied for the selective oxidation of HMF in toluene and DMF as shown in Table S1.[39–48] Other catalysts reported to be active for DFF formation include metal oxides containing Mn, V, Cu, Co, and

Table 1. Aerobic oxidation of HMF and HMF-acetal over supported Ru catalysts.[a]

Entry	Substrate	Concentration (wt%)	Conversion (%)	Product yield (%) DFF	FFCA	Byproducts	Carbon balance (%)
1	HMF-acetal	10	90.4±8.0	77.6±5.3	2.7±0.2	10.1±3.0	89.9±3.0
2		30	95.0±3.0	79.3±1.9	2.6±0.6	13.1±4.0	86.9±4.0
3		50	94.2±1.0	84.0±1.8	2.6±0.3	7.6±1.0	92.4±1.0
4		70	96.7±1.8	53.3±1.4	1.9±1.2	41.5±0.9	58.5±0.9
5	HMF	10	96.4±1.8	52.3±1.5	15.1±2.8	29.0±1.3	71.0±1.3
6		30	93.1±4.8	53.3±3.0	14.5±4.1	25.3±1.1	74.7±1.1
7		50	91.2±1.1	21.2±2.0	6.7±2.9	63.3±5.0	36.7±5.0
8		70	99.4±1.1	4.6±2.3	0.4±0.9	94.4±3.1	5.6±3.1

[a]Reaction conditions: substrate, HMF-acetal or HMF (0.1-0.7 g); solvent, DMF (0.3-0.9 g); catalyst, Ru/γ-Al_2O_3 (substrate to Ru ratio of 20 (wt./wt.)); oxygen pressure, 0.5 MPa; temp., 383 K; time, 300 min.

Fe [49–53], while also metal-free and nitrogen-doped carbon catalysts show significant potential for this reaction.[54] Despite high DFF yields, all reactions in the previous works were only studied using dilute HMF solutions (< 10 wt% HMF) as shown in Table S1. This is most likely due to severe byproduct formation, which proceeds predominantly in concentrated solutions as exemplified in the aerobic oxidation of 10 wt% HMF in water and methanol over a CeO_2-supported Au catalyst.[55,56]

Byproduct formation is a serious issue for the catalytic valorization of lignocellulose biomass, which cannot be simply controlled by optimization of the reaction conditions (temperature, substrate concentration, type of catalyst, etc). To suppress byproduct formation in concentrated solutions, we have developed a protection strategy of the highly reactive formyl group in HMF with 1,3-propanediol.[55,56] Acetalization of the formyl group with 1,3-propanediol forms a six-membered ring acetal, which shows high stability against side reactions during aerobic oxidation and oxidative esterification to synthesize FDCA and its alkyl carboxylate derivatives. Such protection strategies are recently regarded to be effective for biomass conversion as biomass-derived intermediates usually have highly reactive functional groups that are easily involved in side reactions.[57–61]

Herein, we employed the acetal protection strategy for the selective production of DFF from HMF. We oxidized the acetal form of HMF with 1,3-propanediol (HMF-acetal) using carbon-, γ-Al_2O_3-, ZrO_2-, and hydrotalcite (HT)-supported Ru catalysts in DMF as a solvent, because the combination of supported Ru catalysts and DMF has been effective for selective DFF formation (> 90% selectivity) in dilute HMF solutions (Table S1).[39,44,45] HMF and HMF-acetal in various concentrations (10 wt% to 70 wt%) were oxidized to clarify the effect of the acetal functionality on the product distribution. Kinetic studies were used to evaluate the electron-donating effect of the acetal functionality toward the oxidation rate for -CH_2OH by comparison with other reference furan compounds. Furthermore, a regeneration strategy was developed for the used Ru catalyst.

Results and Discussion

Aerobic oxidation of HMF and HMF-acetal

A previous study[39] reported that inert or weakly amphoteric supports are well-suited for HMF oxidation to DFF as HMF degrades rapidly in contact with strongly acidic or basic supports, and Ru/C is found to be the most optimal catalyst. In this paper, we also prepared supported Ru catalysts with inert (C and SiO_2) and amphoteric oxide (γ-Al_2O_3, HT, and ZrO_2) supports and examined them in aerobic oxidation of HMF-acetal. All supported Ru catalysts were characterized by XRD (Figure S1). No distinct diffraction features related to Ru were observed for Ru/γ-Al_2O_3 and Ru/C (Figures S1 (B), and (E)), while Ru/SiO_2, Ru/HT, and Ru/ZrO_2 exhibited broad features assignable to metallic Ru (Figures S1 (A), (C), and (D)). The former samples likely contain highly dispersed and metallic Ru nanoparticles, which cannot be detected by XRD due to their small size. The average size of the metallic Ru nanoparticles in Ru/SiO_2, Ru/HT, and Ru/ZrO_2, estimated by use of the Scherrer equation (using the Ru (101) reflection), was 3.8 nm, 6.3 nm, and 12.3 nm, respectively. The original layered structure of the HT support was completely lost during the reduction step (Figure S1(C)).[62] The XRD pattern of the resulting Ru/HT catalyst did not contain features associated with the original HT support, which means that the Ru nanoparticles are situated on a mixed oxide of MgO and Al_2O_3.

These catalysts were preliminarily examined in aerobic oxidation of the HMF-acetal using a 10 wt% HMF-acetal solution (Figure S2). Here, Ru/γ-Al_2O_3 vastly outperformed Ru/C, which differs from the results reported by the previous study.[39] Ru/ZrO_2, Ru/SiO_2 and Ru/HT performed fairly equal in terms of DFF yield and selectivity but these three catalysts were also less active than Ru/γ-Al_2O_3. The lower activities of Ru/ZrO_2, Ru/SiO_2 and Ru/HT can instead be explained by the difference in Ru particle size. Average particle sizes of Ru/SiO_2, Ru/HT, and Ru/ZrO_2 were 3.8-12.3 nm, respectively, which were all significantly larger than that of Ru/γ-Al_2O_3 (Figure S3(A), approximately 1.5 nm estimated by TEM observation). Ru/γ-Al_2O_3 was therefore selected for further optimization studies. DMF was also selected as an appropriate solvent and used throughout this study (see a solvent screening in page S6 of the supporting).

Ru/γ-Al_2O_3 was used to examine the performance in the aerobic oxidation of HMF and HMF-acetal as a function of the substrate concentration. The oxidation reaction was conducted at 383 K for 300 min in DMF under 0.5 MPa O_2 pressure with a substrate to Ru ratio of 20 wt/wt. Table 1 summarizes the catalytic performance data at various HMF-acetal concentrations (entries 1-4). All acetal moieties were completely removed from the reaction products (DFF-acetal and FFCA-acetal) and the

substrate (HMF-acetal) during HPLC analysis involving the use of a diluted H_2SO_4 eluent.[55] However, kinetic studies in the following section, in which analysis relied on a combination of HPLC and ^{1}H NMR, revealed that deprotection of HMF-acetal under the given reaction conditions was negligible. This means that DFF and FFCA were only present in their acetal form during the reaction. For the sake of brevity, the yields of DFF-acetal and FFCA-acetal are nevertheless expressed as "DFF yield" and FFCA yield" in Table 1. The conversion values estimated by HPLC therefore reflect the HMF-acetal conversion. Ru/γ-Al_2O_3 afforded DFF in 77.6% yield at 90.4% conversion in a 10 wt% HMF-acetal solution (entry 1). FFCA was obtained as a minor product in a yield of only 2.7%, which means that the oxidation of the formyl group in DFF is effectively suppressed under the given reaction conditions, which is due to the absence of water in the reaction medium (Scheme S1). High DFF yields (~ 80%) could also be obtained in 30 wt% and 50 wt% solutions (entries 2 and 3). The difference between HMF-acetal conversion and the sum of identified products (DFF and FFCA) is very small in these experiments, indicating that the amount of oligomerized products that cannot be detected, was very low, even at an HMF-acetal concentration as high as 50 wt%. However, a further increase in the HMF-acetal concentration to 70 wt% (entry 4) led to a lower DFF yield of 53.3% with a large increase in byproduct yield (41.5%). When HMF-acetal was replaced by HMF, the dependence of the product distribution on substrate concentration was very different. DFF yield was moderate (52.3%) at an HMF concentration of only 10 wt% (entry 5). The formation of FFCA in 15.1% yield and a large amount of undetectable byproducts in 29.0% yield point to substantial contributions of the over-oxidation of the formyl group in DFF and condensation reactions of HMF and DFF into oligomerized products. While similar results were obtained in a 30 wt% HMF solution (entry 6), the formation of byproducts became dominant upon a further increase of the HMF concentration, affording DFF yields of 21.2% at 50 wt% substate concentration (entry 7) and 4.6% at 70 wt% substrate concentration (entry 8). These results demonstrate that the protection of formyl moiety with 1,3-propanediol can facilitate the selective synthesis of DFF in concentrated solutions.[55] HMF-acetal provided significant advantage in DFF formation using concentrated solutions compared to HMF. However, the values of carbon balance are approximately 90% (entries 1-3), which is due to humin-type byproduct formation. Such byproducts are stabilized on the catalyst surface and influence the reusability of the Ru/Al_2O_3 catalyst (*vide infra*).

Kinetic studies on aerobic oxidation of HMF and HMF-acetal. Reaction pathways for the oxidation of HMF and HMF-acetal were investigated at 383 K under 0.5 MPa O_2 atmosphere using Ru/γ-Al_2O_3 as the catalyst and a substrate concentration of 50 wt%. Figure 1 shows time courses for HMF conversion and product yields. Kinetic traces were fitted using pseudo-first order-reaction kinetics. HMF was oxidized to DFF, while the further conversion of DFF to FFCA was small. The reaction rate constant for DFF formation (k_1 = 0.84 h^{-1}) is much larger than that for FFCA formation (k_2 = 0.05 h^{-1}). Oxidation of the formyl group to the carboxylic acid is largely suppressed under the given reaction conditions as evidenced by the absence of HMFCA and FDCA as well as by the very small amount of FFCA formed (see Scheme S1). The high selectivity to DFF can be explained by the aprotic nature of the DMF solvent, which prevents the hydration of the aldehyde moiety to the geminal diol intermediate prior to its oxidation to the corresponding carboxylic acid (Scheme S1).[63] The DFF yield reached a maximum after 60 min and then decreased gradually with time, accompanied by increasing levels of oligomerized byproducts. Fitting of the kinetic traces suggests that these byproducts are formed from both HMF and DFF with similar reaction rate constants, i.e., 0.30 h^{-1} (k_3) and 0.24 h^{-1} (k_4), respectively.

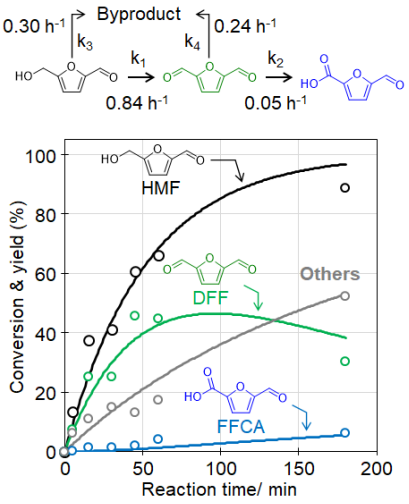

Figure 1. Time course for DFF formation from HMF: HMF 0.5 g; DMF, 0.5 g; Ru/γ-Al_2O_3 catalysts, 0.5 g (substrate to Ru ratio of 20 (wt./wt.)); oxygen pressure, 0.5 MPa; temp., 383 K.

Byproduct formation in HMF oxidation was further evaluated by carrying out two control experiments (Table S2). The reactions were conducted at 383 K for 30 min in the presence of Ru/γ-Al_2O_3 in an inert atmosphere (0.5 MPa N_2) using either a 50 wt% HMF solution or a 50 wt% DFF solution. Approximately 60% of HMF was converted to undetectable byproduct through non-oxidative side reactions (Table S2, entry 1). In contrast, DFF loss under the same reaction conditions was limited to 18.8% (Table S2, entry 2), despite there being no large difference between the rate constants for byproduct formation from HMF and DFF (i.e., k_3 and k_4 in aerobic HMF oxidation, Figure 1). These results imply that DFF degradation is more pronounced under oxidative reaction conditions or in the presence of HMF.

Figure 2 shows time courses for HMF-acetal conversion and product yields, in which kinetic traces were also fitted using pseudo-first order-reaction kinetics. Quantitative analysis using ^{1}H NMR demonstrated that HMF and DFF are present in the acetal form in all reaction mixtures (Figure S4). HMF-acetal conversion and DFF-acetal yield continuously increased with time and reached 81.3% and 73.5% at 60 min and 93.0% and 84.2% at 180 min, respectively. Byproduct formation mainly took place in the initial stage of the reaction (8.8% yield at 30 min) and did not change much afterwards. Oxidation of the formyl group in DFF-acetal hardly proceeded as evident from the small reaction rate constant for FFCA-acetal formation (k_6 = 0.006 h^{-1}), which is an order of magnitude lower than that for FFCA formation in HMF oxidation (k_2 = 0.05 h^{-1}). The acetal moieties in HMF-acetal and DFF-acetal effectively prevent undesired side reactions that lead to condensed products. DFF-acetal was fully retained in the reaction mixture, whereas degradation of free DFF occurred in

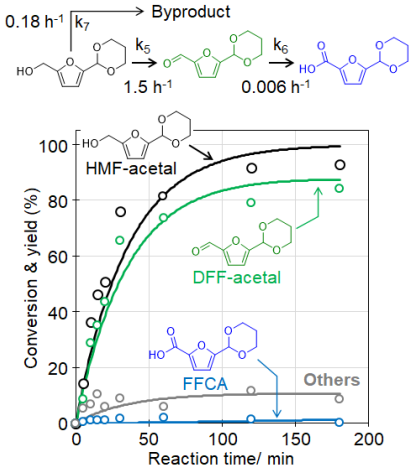

Figure 2. Time course for DFF-acetal formation from HMF-acetal: HMF-acetal 0.5 g; DMF, 0.5 g; Ru/γ-Al_2O_3 catalysts, 0.5 g (Substrate to Ru ratio of 20 (wt./wt.)); oxygen pressure, 0.5 MPa; temp., 383 K

HMF oxidation (k_4 = 0.24 h^{-1} in Figure 1). Byproduct formation from HMF-acetal (k_7 = 0.18 h^{-1}) is approximately half that from HMF (k_3 = 0.30 h^{-1}). Thermal degradation of HMF-acetal and DFF-acetal was also evaluated under an inert atmosphere (Table S2). When the same reactions in entries 1 and 2 of Table S2 were conducted using HMF-acetal and DFF-acetal, both showed very low conversion (< 2%) and minor levels of degradation (entries 3 and 4).

It should be noted that the rate constant for DFF-acetal formation (k_5 = 1.5 h^{-1}, Figure 2) is approximately two times higher than that of DFF formation (k_1 = 0.84 h^{-1}, Figure 1). Such a large difference can explain the efficient production of DFF-acetal in the aerobic oxidation of HMF-acetal. To understand the increase in the reaction rate constant for the oxidation of -CH_2OH to -CHO in the presence of the acetal functional group, we selected two additional substrates, namely HMFCA and furfuryl alcohol. We compared the effect of the functional group (carboxylic acid in HMFCA, hydrogen in furfuryl alcohol, formyl group in HMF, and six-membered acetal group in HMF-acetal) against aerobic oxidation of the hydroxymethyl group over Ru/γ-Al_2O_3 (Figures 1, 2, S5, and S6). Figure 3 summarizes rate constants for a series of substrates. The rate constant for HMF-acetal oxidation is larger (1.5 h^{-1}) compared to oxidation rate constants for furfuryl alcohol (1.2 h^{-1}), HMF (0.84 h^{-1}), and HMFCA (0.03 h^{-1}). There is a correlation between the rate constant and the electron-donating/-withdrawing nature of the functional group. The rate constants were relatively large for the electron-donating acetal functional group in the HMF-acetal. The rate constants decreased with increasing electron-withdrawing character of the functional group (electron-withdrawing property: -COOH in HMFCA > -CHO in HMF > -H in furfuryl alcohol). The presence of electron-donating group most probably facilitated the dissociation of OH and/or CH bonds in -CH_2OH attached to furan ring and enhanced efficient aerobic oxidation to formyl group. A similar effect was observed for the photo-oxidation of substituted benzyl alcohols to benzaldehyde.[64]

In sharp contrast to alcohol oxidation (-CH_2OH), similar reaction rate constants were obtained for aldehyde oxidation to carboxylic acid in three substrates (HMF-acetal, k_6 = 0.006 h^{-1} in Figure 2; HMFCA, k_2 = 0.006 h^{-1} in Figure S5; furfuryl alcohol, k_2 = 0.006 h^{-1} in Figure S6), suggesting no influence of the type of functional group on the reaction rate constant. The formation of carboxylic acid from aldehyde under the reaction conditions requires water to produce geminal diol intermediate as shown in Scheme S1. All oxidation reactions were conducted in non-aqueous solutions, which successfully suppressed undesirable oxidation to the carboxylic acid. Aldehyde oxidation to carboxylic acid forming FFCA (Figure 1) is also nearly absent during HMF oxidation, but its rate constant (k_2 = 0.05 h^{-1}) is an order of magnitude higher than for the other three substrates. Relatively large reaction rate constant in HMF oxidation is maybe attributed to water formation in pronounced side reactions leading to the formation of undesirable carboxylic acid by the oxidation of geminal diol intermediate as shown in Scheme S1.

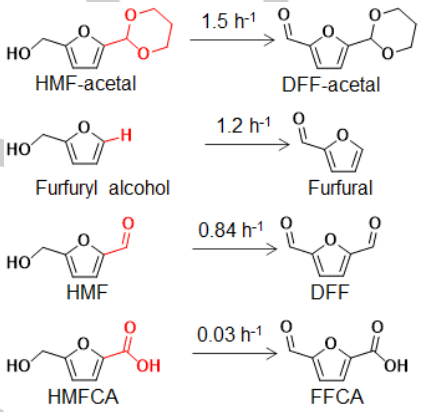

Figure 3. Rate constants for HMF-acetal and reference compounds (furfuryl alcohol, HMF, and HMFCA) in aerobic oxidation: substrate, 0.5 g; DMF, 0.5 g; Ru/γ-Al_2O_3 catalysts, 0.5 g (substrate to Ru ratio of 20 (wt./wt.)); oxygen pressure, 0.5 MPa; temp., 383 K.

Catalyst regeneration

The regeneration of Ru/γ-Al_2O_3 was investigated in the oxidation of HMF-acetal using concentrated solutions (50 wt%), where all reactions were conducted at 383 K for 60 min under 0.5 MPa O_2. After the reaction, the catalyst was recovered by filtration, washed with water (approximately 50 mL), dried at 373 K in air overnight, and then used again in the same reaction (Figure 4A). The DFF-acetal yield decreased from 73.5% to 37.0% in the second run and further to 7.8% in the fifth run. The XRD patterns of fresh and used Ru/γ-Al_2O_3 were similar (Figures S7(a) and S7(b)), implying that catalyst deactivation is not caused by Ru particle growth. It is more likely that deposition of humins blocks part of the surface [45,65] Humin build-up was confirmed by TG-DTA analysis of the used Ru/γ-Al_2O_3, which exhibits a weight loss of approximately 15% in the 423-673 K range (Figure S8(B)). The used catalyst after the fourth reuse was calcined at 773 K for 2 h in air to remove the deposits and reduced at 673 K for 2 h in an H_2 flow (10 mL min^{-1}). This treatment was not effective for the recovery of the original activity. The thus-regenerated catalyst gave a DFF yield of only 5.5% at a conversion of 23.8% in the sixth run under the same reaction conditions. XRD showed that the calcination-reduction treatment leads to growth of Ru nanoparticles (Figure S7(c)), which results in the production of large amounts of undetectable byproduct (18.2%).

Washing with organic solvent mixtures containing acetone, ethanol and toluene was equally ineffective in removing the humin

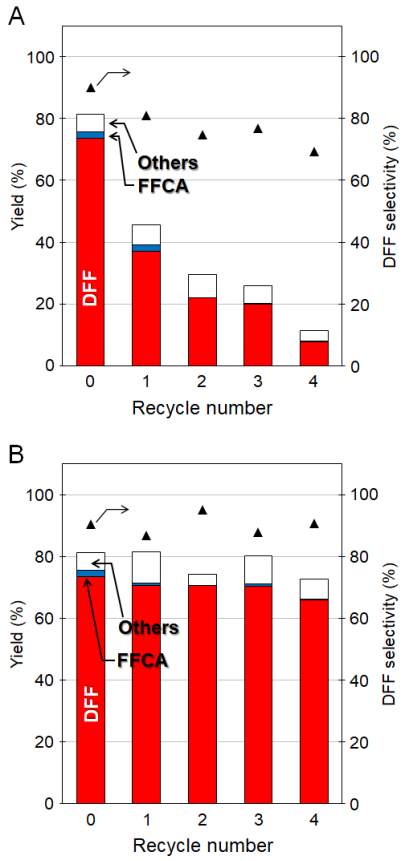

Figure 4. Recyclability of Ru/γ-Al_2O_3 catalyst in aerobic oxidation of HMF-acetal using 50 wt% solutions: (A) washing with water and (B) sonication in aqueous NaOH (pH = 12) solution. Reaction conditions: HMF-acetal 0.5 g; DMF, 0.5 g; Ru/γ-Al_2O_3 catalysts, 0.5 g (Substrate to Ru ratio of 20 (wt./wt.)); oxygen pressure, 0.5 MPa; temp., 383 K; time, 60 min.

depositions and recovering original activity (Table S3). Sonication in NaOH solution was therefore adopted to remove organic deposits from the surface of Ru nanoparticles.[45] The used catalyst was dispersed in an aqueous NaOH solution (pH = 12, 50 mL) and sonicated at room temperature for 10 min. This treatment was repeated three times with refreshing the solution at every cycle. After the final step, the catalyst was recovered by filtration, washed with water, dried in an oven overnight, and then used again in the DFF-acetal oxidation reaction. Figure 4B shows the catalytic activity of fresh and regenerated Ru/γ-Al_2O_3 catalysts. The HMF-acetal conversion of 70–80% and DFF-acetal selectivity of approximately 80% were maintained for five cycles. We also characterized the 4-times reused Ru/γ-Al_2O_3 catalyst after regeneration by TG-DTA, XRD, TEM, and XPS. The TG-DTA profile of the used catalyst in Figure S8(C) is similar to that of the fresh catalyst in Figure S8(A), showing that the NaOH treatment is effective in removing organic deposits. The XRD patterns of fresh and used-generated catalysts in Figures S7(a) and S7(d) demonstrate that the NaOH treatment did not lead to Ru nanoparticle growth. This finding is also corroborated by TEM analysis of fresh and used catalysts, showing a predominance of 1-2 nm sized Ru nanoparticles in both catalysts (Figure S3). The oxidation state of Ru nanoparticle for fresh and used catalysts was investigated by XPS (Figure S9). There was no significant difference in the ratio of metallic Ru and oxidized Ru (Ru^{n+}) between fresh and used catalysts (Table S4). Finally, leaching of oxidized Ru species during the regeneration treatment using NaOH solutions was evaluated by ICP-AES analysis. NaOH solutions after sonication with the used catalyst contained only trace level of Ru (~0.005%), demonstrating that leaching of the supported Ru nanoparticles is nearly negligible. All these results evidence that aerobic oxidation of HMF-acetal with 1,3-propanediol using Ru/γ-Al_2O_3 is a promising strategy for the efficient and scalable production of DFF in excellent yields using concentrated solutions.

Conclusion

A facile reaction system to produce DFF from HMF was developed using concentrated HMF-acetal solutions and a Ru/γ-Al_2O_3 catalyst. Acetal protection of the formyl group in HMF prevents side reactions in concentrated solutions during aerobic oxidation. Under optimized conditions, HMF-acetal was oxidized at a concentration of 50 wt% in DMF using Ru/γ-Al_2O_3 at an HMF-acetal/Ru mass ratio of 20 at 383 K under 0.5 MPa O_2 pressure. After 5 h, a high DFF yield of 84.0% was obtained. Under comparable conditions, oxidation of HMF yielded only 21.2% of DFF. Deposition of humin-type organic compounds during the reactions resulted in a substantial decrease of the original activity of Ru/γ-Al_2O_3 in reuse experiments. Sonication of the used catalyst in NaOH solution removed the deposits and fully recovered the activity, allowing efficient regeneration for at least 4 times without significant loss of activity. DFF production using concentrated solutions in this study is significantly distinct from those in previous reports in terms of productivity as well as the energy consumption for the work-up process. The benefits of working with concentration substrate concentrations are a smaller reactor size and lower energy cost for recycling the organic solvent by evaporation and distillation. Thus, a novel chemocatalytic route to DFF, which is a precursor to building blocks for polyamides and polyesters, has been developed.

Experimental Section

Materials

Ru/γ-Al_2O_3, DMF, hydrotalcite (HT), and ZrO_2 were purchased from FUJIFILM Wako Pure Chemical Corporation. HMF, 2-furoic acid, and furfural were procured from Sigma-Aldrich. DFF, FFCA, furfuryl alcohol, and FDCA were obtained from Tokyo Chemical Industry. HMFCA was purchased from Combi-Blocks Inc. Ruthenium (III) nitrosyl nitrate solution (1.5 wt% of Ru) was procured from Strem Chemicals. Aerosil-380 (SiO_2) and activated carbon (AC) were obtained from Evonik industries and Ajinomoto Fine-Techno Corporation, respectively.

Catalyst preparation

Ru/HT, Ru/C, Ru/SiO_2, and Ru/ZrO_2 catalysts with Ru loading of 5 wt% were prepared by incipient wetness impregnation using ruthenium (III) nitrosyl nitrate. HT, SiO_2, ZrO_2, or AC was added to an aqueous solution containing ruthenium (III) nitrosyl nitrate precursor. After stirring the mixture at room temperature and subsequent vacuum evaporation of water at 373 K, the solids recovered were dried at 393 K overnight in air and then reduced in H_2 at a flow of (10 mL min^{-1}) at 673 K for 2 h (10 K min^{-1}). Ru/γ-Al_2O_3 was used as received.

Catalyst characterization

Powder X-ray diffraction (XRD) patterns were obtained from an X-ray diffractometer (Rigaku, Ultima IV) using Cu Kα radiation (40 kV, 20 mA) over the 2θ range of 10°−90°. Adsorption isotherms were acquired from a

Belsorp mini II (Microtrac MRB). The BET equation was used to estimate the specific surface areas (P/P_0 = 0.05−0.30). X-ray photoelectron spectroscopy (XPS) spectra were acquired using a JEOL JPC-9010MC instrument at pass energy of 20 eV using the Mg Kα line. Charge correction was based on the position of C 1s (284.6 eV). Transmission electron microscope (TEM) images were obtained using a microscope (JEM-2100F JEOL Ltd.) without metal deposition on the sample. Possible metal leaching as a result of the alkaline washing procedure of spent catalysts was analyzed by inductively coupled plasma atomic emission spectroscopy (ICP-AES; ICPE-9000, Shimadzu). Thermogravimetric analyses (TGA) were performed on a Rigaku Thermo plus TG 8121 apparatus in the temperature range from room temperature to 1273 K at a heating rate of 10 K min^{-1} under flowing Air (50 mL min^{-1}).

Aerobic oxidation of HMF and HMF-acetal

Catalytic activity was tested in a 10 ml SUS-316 stainless steel batch reactor equipped with a PTFE liner. 0.1-0.7 g of the substrate (HMF or HMF-acetal prepared according to a previous paper[55]), 0.3-0.9 g of DMF, and 0.1-0.7 g of the Ru catalyst were charged into the reactor, which was subsequently pressured with oxygen to 0.5 MPa and heated in an oil bath at 383 K, where substrate to catalyst (Ru) ratio on mass basis were kept constant at 20 in all reactions. After a specified reaction period, the reactor was cooled to room temperature, and products were analyzed by High-Performance Liquid Chromatography (HPLC). The quantification of HMF, DFF, FFCA, and FDCA was conducted by HPLC (SHIMADZU, Japan) consisting of a RID-10A detector, a UV-SPD-20A detector, and an Aminex HPX-87H ion column (column temp., 308 K). A diluted H_2SO_4 solution (5 mM) was used as the eluent at a flow rate of 0.5 mL min^{-1}. The retention times for furaldehyde, HMF, furoic acid, DFF, FFCA, HMFCA, FDCA, and furfuryl alcohol were 67.0, 43.3, 42.5, 54.4, 30.0, 27.0, 21.0, and 15.6 min, respectively. As reported in previous papers, HMF-acetal, DFF-acetal, or FFCA-acetal were quantitatively converted to HMF, DFF, or FFCA, respectively, during HPLC measurement.[55]

Acknowledgements

This work was supported by JST-MIRAI program (Grant number JPMJMI19E3), Japan. A part of this work was also supported by JSPS Grant-in-Aid for Transformative Research Areas (A) "Hyper-Ordered Structures Science (20H05879)", JSPS Fostering Joint International Research (B) (18KK0135), and the Cooperative Research Program of Institute for Catalysis, Hokkaido University (20A1002).

Keywords: Biomass • Diformylfuran • Heterogeneous catalyst • (5-hydroxymethyl)furfural • Oxidation

[1] J. N. Chheda, G. W. Huber, J. A. Dumesic, *Angew. Chem. Int. Ed.* **2007**, *46*, 7164–7183.
[2] J. J. Bozell, G. R. Petersen, *Green Chem.* **2010**, *12*, 539–55.
[3] G. W. Huber, S. Iborra, A. Corma, *Chem. Rev.* **2006**, *106*, 4044–4098.
[4] A. Corma Canos, S. Iborra, A. Velty, *Chem. Rev.* **2007**, *107*, 2411–2502.
[5] I. Delidovich, P. J. C. Hausoul, L. Deng, R. Pfützenreuter, M. Rose, R. Palkovits, *Chem. Rev.* **2016**, *116*, 1540–1599.
[6] C. Li, X. Zhao, A. Wang, G. W. Huber, T. Zhang, *Chem. Rev.* **2015**, *115*, 11559–11624.
[7] F. H. Isikgor, C. R. Becer, *Polym. Chem.* **2015**, *6*, 4497–4559.
[8] H. Zhao, J. E. Holladay, H. Brown, Z. C. Zhang, *Science.* **2007**, *316*, 1597–1600.
[9] E. A. Pidko, V. Degirmenci, R. A. Van Santen, E. J. M. Hensen, *Angew. Chem. Int. Ed.* **2010**, *49*, 2530–2534.
[10] E. Nikolla, Y. Román-Leshkov, M. Moliner, M. E. Davis, *ACS Catal.* **2011**, *1*, 408–410.
[11] K. Nakajima, Y. Baba, R. Noma, M. Kitano, J. N. Kondo, S. Hayashi, M. Hara, *J. Am. Chem. Soc.* **2011**, *133*, 4224–4227.
[12] R. Noma, K. Nakajima, K. Kamata, M. Kitano, S. Hayashi, M. Hara, *J. Phys. Chem. C* **2015**, *119*, 17117–17125.
[13] C. Yue, G. Li, E. A. Pidko, J. J. Wiesfeld, M. Rigutto, E. J. M. Hensen, *ChemSusChem* **2016**, *9*, 2421–2429.
[14] G. Li, E. A. Pidko, E. J. M. Hensen, K. Nakajima, *ChemCatChem* **2018**, *10*, 4084–4089.
[15] O. Casanova, S. Iborra, A. Corma, *ChemSusChem* **2009**, *2*, 1138–1144.
[16] O. Casanova, S. Iborra, A. Corma, *J. Catal.* **2009**, *265*, 109–116.
[17] N. K. Gupta, S. Nishimura, A. Takagaki, K. Ebitani, *Green Chem.* **2011**, *13*, 824–827.
[18] M. Sajid, X. Zhao, D. Liu, *Green Chem.* **2018**, *20*, 5427–5453.
[19] E. Hayashi, Y. Yamaguchi, K. Kamata, N. Tsunoda, Y. Kumagai, F. Oba, M. Hara, *J. Am. Chem. Soc.* **2019**, *141*, 899–900.
[20] Y. Takeda, M. Tamura, Y. Nakagawa, K. Okumura, K. Tomishige, *Catal. Sci. Technol.* **2016**, *6*, 5668–5683.
[21] M. Tamura, K. Tokonami, Y. Nakagawa, K. Tomishige, *Chem. Commun.* **2013**, *49*, 7034–7036.
[22] S. T. Thompson, H. H. Lamb, *ACS Catal.* **2016**, *6*, 7438–7447.
[23] J. J. Wiesfeld, M. Kim, K. Nakajima, E. J. M. Hensen, *Green Chem.* **2020**, *22*, 1229–1238.
[24] T. Buntara, S. Noel, P. H. Phua, I. Melián-Cabrera, J. G. De Vries, H. J. Heeres, *Angew. Chem. Int. Ed.* **2011**, *50*, 7083–7087.
[25] X. Kong, R. Zheng, Y. Zhu, G. Ding, Y. Zhu, Y. W. Li, *Green Chem.* **2015**, *17*, 2504–2514.
[26] J. Chen, R. Liu, Y. Guo, L. Chen, H. Gao, *ACS Catal.* **2015**, *5*, 722–733.
[27] Y. Nakagawa, K. Takada, M. Tamura, K. Tomishige, *ACS Catal.* **2014**, *4*, 2718–2726.
[28] Y. Nakagawa, K. Tomishige, *Catal. Commun.* **2010**, *12*, 154–156.
[29] S. Yao, X. Wang, Y. Jiang, F. Wu, X. Chen, X. Mu, *ACS Sustain. Chem. Eng.* **2014**, *2*, 173–180.
[30] T. Buntara, I. Melián-Cabrera, Q. Tan, J. L. G. Fierro, M. Neurock, J. G. De Vries, H. J. Heeres, *Catal. Today* **2013**, *210*, 106–116.
[31] M. J. Gilkey, A. V. Mironenko, L. Yang, D. G. Vlachos, B. Xu, *ChemSusChem* **2016**, *9*, 3113–3121.
[32] D. Pingen, J. B. Schwaderer, J. Walter, J. Wen, G. Murray, D. Vogt, S. Mecking, *ChemCatChem* **2018**, *10*, 3027–3033.
[33] Y. Xu, X. Jia, J. Ma, J. Gao, F. Xia, X. Li, J. Xu, *Green Chem.* **2018**, *20*, 2697–2701.
[34] K. Zhou, H. Liu, H. Shu, S. Xiao, D. Guo, Y. Liu, Z. Wei, X. Li, *ChemCatChem* **2019**, *11*, 2649–2656.
[35] G. Liang, A. Wang, L. Li, G. Xu, N. Yan, T. Zhang, *Angew. Chem. Int. Ed.* **2017**, *56*, 3050–3054.
[36] H. Qi, F. Liu, L. Zhang, L. Li, Y. Su, J. Yang, R. Hao, A. Wang, T. Zhang, *Green Chem.* **2020**, *22*, 6897–6901.
[37] W. M, R. B, *Macromol. Rapid Commun.* **2016**, *37*, 1391–1413.
[38] J. M. García, F. C. García, F. Serna, J. L. de la Peña, *Prog. Polym. Sci.* **2010**, *35*, 623–686.
[39] J. Nie, J. Xie, H. Liu, *J. Catal.* **2013**, *301*, 83–91.
[40] S. E. Davis, L. R. Houk, E. C. Tamargo, A. K. Datye, R. J. Davis, *Catal. Today* **2011**, *160*, 55–60.
[41] Y. Zhu, M. Shen, Y. Xia, M. Lu, *Catal. Commun.* **2015**, *64*, 37–43.
[42] Z. Zhang, Z. Yuan, D. Tang, Y. Ren, K. Lv, B. Liu, *ChemSusChem* **2014**, *7*, 3496–3504.
[43] D. K. Mishra, J. K. Cho, Y. J. Kim, *J. Ind. Eng. Chem.* **2018**, *60*, 513–519.
[44] A. Takagaki, M. Takahashi, S. Nishimura, K. Ebitani, *ACS Catal.* **2011**, *1*, 1562–1565.
[45] C. A. Antonyraj, J. Jeong, B. Kim, S. Shin, S. Kim, K. Y. Lee, J. K. Cho, *J. Ind. Eng. Chem.* **2013**, *19*, 1056–1059.
[46] K. Ghosh, R. A. Molla, M. A. Iqubal, S. S. Islam, S. M. Islam, *Appl. Catal. A Gen.* **2016**, *520*, 44–52.
[47] J. Chen, J. Zhong, Y. Guo, L. Chen, *RSC Adv.* **2015**, *5*, 5933–5940.
[48] Y. Liu, T. Gan, Q. He, H. Zhang, X. He, H. Ji, *Ind. Eng. Chem. Res.* **2020**, *59*, 4333–4337.
[49] S. Biswas, B. Dutta, A. Mannodi-Kanakkithodi, R. Clarke, W. Song, R. Ramprasad, S. L. Suib, *Chem. Commun.* **2017**, *53*, 11751–11754.
[50] S. Wen, K. Liu, Y. Tian, Y. Xiang, X. Liu, D. Yin, *Processes* **2020**, *8*, 1–8.
[51] R. Fang, R. Luque, Y. Li, *Green Chem.* **2016**, *18*, 3152–3157.
[52] F. Nocito, M. Ventura, M. Aresta, A. Dibenedetto, *ACS Omega* **2018**, *3*, 18724–18729.
[53] Z. Yuan, B. Liu, P. Zhou, Z. Zhang, Q. Chi, *Catal. Sci. Technol.* **2018**, *8*, 4430–4439.
[54] Y. Ren, Z. Yuan, K. Lv, J. Sun, Z. Zhang, Q. Chi, *Green Chem.* **2018**, *20*, 4946–4956.
[55] M. Kim, Y. Su, A. Fukuoka, E. J. M. Hensen, K. Nakajima, *Angew. Chem. Int. Ed.* **2018**, *57*, 8235–8239.
[56] M. Kim, Y. Su, T. Aoshima, A. Fukuoka, E. J. M. Hensen, K. Nakajima, *ACS Catal.* **2019**, *9*, 4277–4285.
[57] L. Shuai, M. T. Amiri, Y. M. Questell-Santiago, F. Héroguel, Y. Li, H. Kim, R. Meilan, C. Chapple, J. Ralph, J. S. Luterbacher, *Science* **2016**, *354*, 329–333.
[58] W. Lan, M. T. Amiri, C. M. Hunston, J. S. Luterbacher, *Angew. Chem. Int. Ed.* **2018**, *57*, 1356–1360.
[59] Y. M. Questell-Santiago, R. Zambrano-Varela, M. Talebi Amiri, J. S. Luterbacher, *Nat. Chem.* **2018**, *10*, 1222–1228.

[60] Y. M. Questell-Santiago, J. H. Yeap, M. Talebi Amiri, B. P. Le Monnier, J. S. Luterbacher, *ACS Sustain. Chem. Eng.* **2020**, *8*, 1709–1714.
[61] X. Luo, Y. Li, N. K. Gupta, B. Sels, J. Ralph, L. Shuai, *Angew. Chem. Int. Ed.* **2020**, *59*, 11704–11716.
[62] K. Ebitani, K. Motokura, K. Mori, T. Mizugaki, K. Kaneda, *J. Org. Chem.* **2006**, *71*, 5440–5447.
[63] S. E. Davis, B. N. Zope, R. J. Davis, *Green Chem.* **2012**, *14*, 143–147.
[64] I. Krivtsov, M. Ilkaeva, E. I. García-López, G. Marcì, L. Palmisano, E. Bartashevich, E. Grigoreva, K. Matveeva, E. Díaz, S. Ordóñez, *ChemCatChem* **2019**, *11*, 2713–2724.
[65] H. F. Ren, X. Luo, K. Zhang, Q. Cai, C. L. Liu, W. S. Dong, *J. Porous Mater.* **2020**, *27*, 1003–1012.

WILEY-VCH

Entry for the Table of Contents

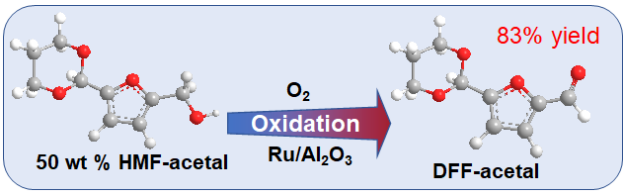

WILEY-VCH